

# Pani Modified Ag NPs Fluorescence Sensor for Detection of Nitrate Ion

Abdu Hussen Ali (✉ [abdelmelik9@gmail.com](mailto:abdelmelik9@gmail.com))

---

## Research Article

**Keywords:** Fluorescent, Nanocomposite, Nitrate ion, Polyaniline, Quenching, Sensor, Toxicity

**Posted Date:** March 15th, 2022

**DOI:** <https://doi.org/10.21203/rs.3.rs-1449278/v1>

**License:**  This work is licensed under a Creative Commons Attribution 4.0 International License.

[Read Full License](#)

---

**PANI MODIFIED Ag NPs FLUORESCENCE SENSOR FOR DETECTION OF  
NITRATE ION**

**Abdu Hussien Ali**

Department of Chemistry, College of Natural and Computational Sciences, Mekdela Amba  
University; P. O. Box 32, Tuluawliya, Ethiopia. **Emails: [abdelmelik9@gmail.com](mailto:abdelmelik9@gmail.com)**

## ABSTRACT

*Nitrate is one of the major environmental problems in today's world, which affect human health and welfare, and hinders the sustainable development of both society and the economy. Therefore, the growth of sensor based on decorated noble metal nanoparticles (NPs) such as Ag have been attracted great attention for their convenience of simple operation, excellent absorption and scattering (extinction) properties in recent years. A new and simple fluorometric sensing probe based on polyaniline functionalized AgNPs for  $\text{NO}_3^-$  ion detection was developed by polymerization method. It has been successfully synthesized by in-situ polymerization method. The structural and optical properties of the as-synthesized nanocomposites were characterized by using, Fourier- Transform Infrared spectroscopy (FT-IR), powder X-ray diffraction (XRD), Photoluminescence (PL) and UV-Vis spectroscopy. In the absence of nitrate ion, the PANI/Ag exhibit high fluorescence intensity. Yet, the strong coordination of the basic sites with nitrate ion, causes fluorescence intensities quenching through static quenching leading to the qualitative and quantitative detection of nitrate ion. Factor affecting the detection system such as pH and concentration are optimized. Also, the developed PANI modified Ag sensor exhibits high selectivity and sensitive toward nitrate ion with detection limit of  $8.9 \times 10^{-4}$  M. The practical use of the sensor as well tested by spiked with different concentration of nitrate ion solutions on cabbage samples. The result signposted a good linear relation between  $F_0/F$  and the spiked concentrations of nitrate ion with coefficient of regression  $R^2 = 0.991$  ( $n= 3$ ) and also confirms that the found values is agreed well with the spiked amount.*

**Keyword:** Fluorescent, Nanocomposite, Nitrate ion, Polyaniline, Quenching, Sensor, Toxicity

## 1. INTRODUCTION

Chemical pollution is one of the major environmental problems in today's world, since polluted environment poses a threat to human health and welfare, and hinders the sustainable development of both society and the economy. The presence of chemical toxins, heavy metals, inorganic and organic pollutants in water, food and soil, due to either natural or artificial processes result environmental problem [1]. Nitrate is a common chemical compound in the nature, and is widely found in soils, waters, and foods. It has been classified as an inorganic nitrogenous compound, which can cause disease and become a threat to human health. The nitrate can be found naturally in water, soil, and food; thus, it can be easily consumed by humans. Due to the excess of nitrate, symptoms such as abdominal pain and diarrhea have also been observed in human [2] and disruption of endocrine functioning of the thyroid gland are some of the prominent ill effects of nitrates [3].

Therefore, it needs to be monitored constantly to safeguard the supply of clean drinking water and food to the public, and to control the impact on the environment and the ecosystem. Conventional analytical techniques for nitrate ion detection have been developed, such as ion chromatography (IC), Raman spectroscopy [4], atomic absorption spectrometry (AAS) [5] and inductively coupled plasma optical emission spectrometry (ICP-OES) [6]. These methods require high-cost analytical instruments developed for use in the laboratories. The necessary sample collection, transportation and pre-treatment is time-consuming and a potential source of error. Recently, the combination of nanotechnology, chemistry, physics and biology, has allowed the development of ultrasensitive detection and imaging methods, including applications in electronic, magnetic, environmental, pharmaceutical, cosmetic, energy, optoelectronic, catalytic, and material fields [7].

The field of environmental monitoring has seen the application of nanoparticles (NPs) being utilized as functional probes for analyzing toxins, metal ions, and inorganic and organic pollutants [8]. NPs, usually with a size between 1 and 100 nm, display unique properties, mainly due to the strong physical confinement of electrons or holes in the NPs at the nanoscale. From a sensing perspective, the small size of NPs gives them large surface-to-volume ratios, which lead to rapid responses and high sensitivity.

In the fields of chemosensors, the organic sensing materials such as conducting polymers [polyaniline (PANI), polypyrrole (PPy), and polythiophene (PTP), etc.] can show response to target analytes at room temperature or low temperature, which has a convenient operating an attractive prospect [9]. It is very attractive in nanoscience and nanotechnology because of their highly  $\pi$ -conjugated polymeric chains and metal like conductivity. Polyaniline (PANI) is unique among conducting polymers due to its chemical and environmental stability, good redox reversibility, tunable electrical conductivity and optical properties. PANI has three different fundamental forms depending on the method employed for the preparation. The only electrically conducting one is the emeraldine salt form (ES: half oxidized), which is the protonated form of PANI-EB [10]. There have been only a few reports on the application of a simple concept that is fluorescence quenching of polyaniline and its derivatives in optical sensor studies; such as Cu/PANI for chloroform [11] and camphorsulfonic acid doped polyaniline for NO<sub>2</sub> and oxygen gas as chemical sensing based on fluorescence quenching were studied [12].

Chemosensors based on decorated noble metal nanoparticles (NPs) have been also attracted great attention for their convenience of simple operation in recent years by virtue of the excellent absorption and scattering (extinction) properties of Ag NPs, which are impossible in its bulk counterparts. The Ag NPs show many advantages, such as higher extinction coefficients, sharper extinction bands, higher ratio of scattering to extinction and extremely high near-field enhancements. However, there were very few reports on Ag NPs for biosensing applications. This is due to the poor chemical stability of Ag NPs as compared with Au NPs. During the past several years, the use of Ag NPs has been increasing with focus on improving the chemical stabilities. In order to improve the chemical stability, in this work, the synthesis of silver nanoparticles has been carried out using the juice extract of *Citrullus lanatus* (watermelon). The presence of polyphenol in this juice is found to be responsible for the reduction of Ag<sup>+1</sup> to Ag<sup>0</sup> ions and also stabilization of AgNP [13]. Consequently, Ag NPs rapidly gain the popularity. For instance, many groups have started to explore alternative strategies for the development of optical sensors based on their extraordinary optical properties [14].

In addition, the physical properties of NPs (i.e., optical, electronic, magnetic properties) can be fine-tuned through control of their size, composition, shape, and surface chemistry, to generate

highly functional molecular probes. Surface-modified nanoparticles, such as gold and silver NPs (AuNPs/AgNPs) [15], quantum dots (QDs) [16], magnetic NPs (MNPs) [17] and carbon nanotubes [18] can have specific target-binding properties that allow highly selective and sensitive target detection.

In this context, we aimed to establish a new and simple fluorometric sensing probe for  $\text{NO}_3^-$  detection based on polyaniline functionalized AgNPs. We evaluated the PANI functionalized AgNPs and the prepared PANI functionalized AgNPs tend to form complex with  $\text{NO}_3^-$ , which leads to the significant emission change spectrum. These results suggest that, the PANI functionalized AgNPs have great potential for applications in fluorescence sensor and optoelectronic devices.

## **2. EXPERIMENTAL SECTION**

### **2.1. Materials**

Aniline was obtained from Aldrich purified by distillation under reduced pressure prior to use. Sodium dihydrogen phosphate, disodium hydrogen phosphate, hydrochloric acid, Zinc dust, ethanol, ammonium persulphate, Ammonia, Sodium sulphate, Silver nitrate, Sodium bicarbonate, Sodium chloride, Sodium hydroxide, Sodium nitrate were used without purification.

### **2.2. Preparation of juice extract**

The *Citrullus lanatus* was collected from local market and washed with distilled de-ionized water. It was cut into pieces. The inner red portion of the pieces was pasted by mortar pestle. Then, it was filtered using whatman filter paper to get *Citrullus lanatus* juice.

### **2.3. Synthesis of Nanocomposite**

#### **2.3.1. Synthesis of Silver Nanoparticle**

Silver nanoparticles was synthesized as follow, 5 mL of double distilled water was added to 5 mL of pure juice extract to make it 1:1 and it was cooled in ice cold water. The solution was made alkaline (pH 10) by adding NaOH. The whole apparatus was placed on a heating mantle. During heating 6 mL  $3 \times 10^{-3}$  M aqueous silver nitrate solution was added drop wise with continuous

stirring from burette and finally it was heated for 20 min at 70 °C. The color of the solution gradually changed from light pink to reddish yellow. The reddish yellow color indicated the formation of AgNP [19].

### **2.3.2. Synthesis of Polyaniline (PANI) Modified Ag NPs**

PANI/Ag was synthesized by polymerization of aniline in the presence of AgNPs nanocomposite. 1 g of AgNPs powder was added into 20 mL aqueous solution of 0.01 mol aniline monomer and 0.01 mol hydrochloric acid. A 0.01 mol APS was dissolved in a 15 mL distilled water and then added dropwise to the mixture of AgNPs and aniline with stirring in an ice bath. Polymerization proceeded for 5 h. The composite of PANI modified AgNPs was obtained as a precipitate. The precipitate was isolated by filtration, washed with distilled water and ethanol three times, and dried at 70 °C for 3 h. Pure PANI was also synthesized, by using an identical method but without using AgNPs.

### **2.4. Characterization of the Synthesized Nanocomposites**

To determine the characteristic maximum absorption of the as-synthesized samples and their band gaps, UV-Visible absorption spectrophotometer (SANYO SP65) was used in the range of 200-900 nm wavelength. The photoluminescence emission properties were determined using a RF-5301PC spectrofluorometer equipped with a xenon discharge lamp. The crystallite sizes were determined using powder X-ray diffraction (XRD) with X'Pert Pro PANalytical with CuK $\alpha$  radiation ( $\lambda = 1.5405 \text{ \AA}$ ). The data were registered with  $2\theta$  steps of  $0.02^\circ$  and accumulation times of 20 s. FT-IR (Spectrum 65, PerkinElmer) in the range  $4000\text{-}400 \text{ cm}^{-1}$  using KBr pellets was used to assign functional groups of as-synthesized PANI/Ag.

## 2.5. Preparation of Buffers

The 0.1 M phosphate buffer was prepared by weighing approximately 0.8 g of  $\text{NaH}_2\text{PO}_4 \cdot 2\text{H}_2\text{O}$  and 6.5180 g of  $\text{Na}_2\text{HPO}_4$  and dissolving them in water into a 500 mL volumetric flask. It was adjusted using 0.1 M HCl or 0.1 M NaOH to the desired pH. The buffer solution was stored in a fridge at 4 °C [20].

## 2.6. Fluorescence Detection of Nitrate Ion

For fluorescence detection of nitrate ion detection, 1 mg of the PANI/Ag nanocomposite was dissolved in 2.5 mL deionized water and followed by the addition of different molar concentration of nitrate ion and sonicated. After reaction of 5 min at room temperature, 50  $\mu\text{L}$  of the solution was taken into a cuvette and finally, the emission spectra were recorded using fluorescence spectroscopy.

In order to quantify the nitrate ion induced quenching process, the Stern-Volmer quenching constant  $K_{SV}$  was calculated by Stern-Volmer equation:

$$I_0/I = 1 + K_{SV} [Q]$$

Where  $I_0$  and  $I$  are the fluorescence intensities of the sensor in the absence and presence of nitrate ions,  $K_{SV}$  is the Stern-Volmer constant and  $(Q)$  is the molar concentration of nitrate ion.

## 2.7. Optimization of Parameters

### 2.7.1. The Effect of Concentration

The effect of nitrate ion concentration also affects the sensitivity of detection. In order to investigate this effect, 2.5 mL of PBS (0.1 M) was added in to 1 mg of the PANI/Ag nanocomposite, then it was dissolved in 2.5 mL deionized water and followed by the addition of 1, 2, 4, 6, 8, 10, 12 and 14 mM of nitrate ion and sonicated. After reaction of 5 min at room temperature, 50  $\mu\text{L}$  of the solution was taken into a cuvette and finally, the emission spectra were recorded using fluorescence spectroscopy.

### 2.7.2. The Effect of pH

It is common that the pH of a solution can affect the sensitivity and selectivity of a detection. The effect of pH (2-12) of PBS on the PANI/Ag fluorescent sensor in the presence of nitrate ion solution was tested.

## 2.8. Reproducibility and Stability Tests

The reproducibility of the PANI/Ag as the fluorescent sensor was investigated at three repetitions on three batches of the PANI/Ag. A calibration graph was plotted for mean of  $F_0/F$ , ( $F_0$  and  $F$  represented the fluorescence intensity of sensor without and with nitrate ion) Vs. nitrate ion concentration, which a linear range was then determined. Limit of detection was calculated using the following formula;

$$\text{LOD} = \frac{3 \times SD}{K_{SV}}$$

Where LOD are limit of detection, SD are standard deviation from linearity of a graph and  $K_{SV}$  is Stern-Volmer constant calculated from the graph [21].

## 2.9. Selectivity of the Sensor

The  $\text{SO}_4^{2-}$ ,  $\text{Cl}^-$ ,  $\text{OH}^-$  and  $\text{HCO}_3^-$  ions were used to investigate selectivity for nitrate ion of PANI/Ag sensor. The concentration of each anion was 14 mM. The same detection conditions and approach were used as mentioned above.

## 2.10. Recovery Test and Real Samples Analysis

About 5 g of cabbage sample was collected from the local market, Tuluawliya, Ethiopia for nitrate extraction. The cabbage was torn into very small pieces and ground using pistol and mortar. The powder was added into a flask that contains 20 mL of ethanol and sonicated for 15 minutes. The mixture was filtered through a Buchner funnel to separate the liquid from the solid plant material and the liquid part was diluted by adding 5 mL of deionized water. The resultant samples were spiked with different concentrations of nitrate solutions. Then 200  $\mu\text{L}$  of this sample solution was taken and added to PANI/Ag nanocomposite in 2.5 mL deionized water. Finally, fluorescence

emission spectra were recorded after reaction of 5 min at room temperature. The mean percentage recoveries for the nitrate ions were calculated using the following equation:

$$\text{Percentage recovery} = \frac{CE}{CM} \times 100$$

Where CE is the experimental concentrations determined from the calibration curve and CM is the spiked concentrations.

### 3. RESULTS AND DISCUSSION

#### 3.1. Characterization of Modified Ag sensor

##### 3.1.1. FTIR Analysis

As **Figure 1** show that the FTIR spectra of the synthesized nanocomposite samples Polyaniline, Ag NPs and PANI/Ag, in the range 4000-400  $\text{cm}^{-1}$  using KBr pellets. Figure 1(a) shows the FTIR spectra of emeraldine salt PANI. The characteristics peaks are 3435  $\text{cm}^{-1}$  due to N-H stretching mode, 1595  $\text{cm}^{-1}$  due to C=C stretching mode of the quinoid rings, 1384  $\text{cm}^{-1}$  due to C=C stretching mode of benzenoid rings, 1250  $\text{cm}^{-1}$  due to C-N stretching mode and 1120  $\text{cm}^{-1}$  due to N=Q=N, where Q represents the quionoid ring [22]. The presence of the benzenoid and quinoid units is evidence of the emeraldine salt form of PANI. For AgNP the FTIR spectra is described in figure 1 B. The spectrum shows slightly narrower peak at 3458  $\text{cm}^{-1}$  which may be due to hydroxyl (OH) stretching bands which suggests the involvement of the polyphenols in the reduction [23]. The peak at 1635  $\text{cm}^{-1}$  may be due to the presence of carbonyl group (C = O) associated with NH moiety in Riboflavin.

The FTIR spectra of PANI/Ag nanocomposite described in figure 1C, which shows a peaks at 3426  $\text{cm}^{-1}$  are attributed to N-H stretching mode because the range of N-H is between 3300  $\text{cm}^{-1}$  to 3500  $\text{cm}^{-1}$  for amine part of PANI and also due to hydroxyl (OH) stretching bands polyphenols of AgNPs. The small absorption peaks observed at 2918  $\text{cm}^{-1}$  and 2850  $\text{cm}^{-1}$  are due to asymmetric C-H and symmetric C-H stretching vibrations. Most of the observed characteristic peaks of PANI/Ag nanocomposite is the replica of characteristic peaks of PANI. However, the corresponding peaks are shifted to the lower wave numbers, besides their intensities are changed after the Ag nanoparticles addition. The peaks of the PANI around 3435, 1595, 1384 and

1120  $\text{cm}^{-1}$  are shifted to 3426, 1579, 1250 and 1080  $\text{cm}^{-1}$ , respectively. These shifts of characteristic peaks of the PANI may be the result of the interactions between the PANI chains and Ag nanoparticles which affect the electron densities and bond energies of the PANI [24]. The shifting to the lower wave numbers is due to the action of hydrogen bonding between the hydroxyl groups on the surface of Ag nanoparticles and the amine groups in the PANI molecular chains. The characteristic band at 810  $\text{cm}^{-1}$  is corresponding to out-of-plane bending vibration of C–H bond of *p*-disubstituted benzene rings of PANI [25] which confirm that coupling of aniline unit in the surface of AgNPs.

### 3.1.2. XRD Analysis

**Figure 2A** describe the XRD analysis of biosynthesized AgNP to confirm the crystalline nature. From the figure, it shows a characteristics peak at  $31.81^\circ$ ,  $38.20^\circ$ ,  $44.10^\circ$ ,  $46.87^\circ$ ,  $55.2^\circ$ ,  $57.58^\circ$ ,  $64.59^\circ$  and  $77.80^\circ$ . The result indicate that the synthesized AgNP is crystalline and essentially fcc in nature. This result is a good agreement with other works [19]. For pure PANI, figure 2B shows the XRD pattern revealed three weak peaks observed at  $2\theta$  values of  $15.1^\circ$ ,  $20.53^\circ$  and  $25.36^\circ$  corresponding to (111), (100) and (011) plane, which can be attributed to the crystallographic planes for the emeraldine salt form of PANI, which is in a good agreement with other report [26]. The peak at  $15.1^\circ$  is attributed to parallel repeat units of PANI, as well as the peak at  $25.36^\circ$  is assigned to a periodicity caused by H-bonding between PANI chains. The low intensity of the observed peak indicates that the PANI has semi-crystalline nature due to the presence of a benzenoid and quinonoid group [27].

The XRD diffraction of PANI/Ag nanocomposite consist of the major characteristic's diffraction peak of PANI and Ag, yet however the  $2\theta$  values of the peaks slightly shifted. The diffraction peak observed at  $2\theta$  values of  $28.27^\circ$  could be attributed to PANI and  $32.15^\circ$ ,  $39.0^\circ$ ,  $45.43^\circ$ ,  $65.34^\circ$  and  $78.58^\circ$  could be due to AgNP. The increase in the degree of regularity is due to the strong interfacial interaction between the PANI and AgNP.

### 3.1.3. UV-Visible Analysis

The absorbance spectrum of samples of PANI showed the absorption peaks at 290 nm assigned to the benzenoid structure and 380 nm which indicate the principal absorption of the  $\pi$ - $\pi^*$  orbital transitions of the emeraldine form of PANI (**Figure 3A**) as similar with previously investigated [28], almost under similar conditions. PANI can absorb both UV and visible region due to transitions in the PANI molecules. The absorption reveals maximum at about 380 and 550 nm, which originate from the charge transfer excitation from the HOMO level to the LUMO energy level and the  $\pi$ - $\pi^*$  transition [29]. The second peak at 380 nm which also indicates the presence of benzenoid group and lone pair of electrons of nitrogen. This, in turn, leads to  $\pi$ - $\pi^*$  interactions of the molecule and this shows that it is a conducting polymer. For AgNPs a broad absorption band was observed at 405 nm (figure 3B). As the sharp, single peak represents the monodispersity of the extract and water composition.

The UV-Visible spectra of PANI/Ag nanocomposite also show a sharp peak at 280 nm (Figure 3AB) may be assigned to the localized polaron which are characteristics of the protonated PANI, together with extended conducting emeraldine salt form of the sample. The absorption peak red-shifted to the resultant PANI/Ag hybrids suggesting that the recovery of electronic conjugation within the polyaniline occurred. Additionally, the absorption exhibited in the visible region has small absorption peaks at 280 nm, which might be in the relation of the more conductivity of the nanocomposite with the porous of PANI and the peaks at 400 nm specifically indicate the presence of Ag NPs on the surface of PANI.

### 3.2. Mechanism of the Modified Ag Fluorescent Sensor for Nitrate Ion

PANI modified AgNPs exhibited characteristic strong absorption band respectively at 440 nm, and reddish-yellow color in aqueous solution that confirms the formation of AgNPs. The emission intensities of the PANI/Ag nanocomposite were quenched after addition of the nitrate ion. The decrease in the emission intensity can be attributed to the combined effect of decrease in absorbance at the excitation wavelength and due to complex formation between the  $\text{NO}_3^-$  and PANI/Ag. Therefore, the quencher probably involves the donation of electrons from the surface of PANI/Ag nanomaterial to the nitrate ion, deactivating the excited state responsible for fluorescence quenching.

The other possibility for fluorescence intensity quenching occurs due to the most possible interactions between Ag and N sites in PANI/Ag with nitrate ion would be non-covalent interaction like electrostatic or hydrogen bond for chelation (NH/ N-O and Ag-O-N). In addition, the nitrogen-containing groups (nitrogen site) in the PANI/Ag and nitrate ion might be reacted to produce N-nitroso compounds, which results in fluorescence static quenching. This indicates that fluorescence quenching is caused by chemical reactions. The mechanism of quenching at low nitrate ion concentrations may also mostly involves dynamic quenching, which results from collisions between nitrate ions and the PANI/Ag NPs. Static quenching also occurs, but only at higher concentrations.

### **3.3. Optimization of Experimental Conditions**

In order to evaluate the sensitivity of the proposed material, the experimental conditions were optimized including the pH of the buffer solution and concentration of nitrate ion.

#### **3.3.1. The Concentration of Nitrate Ion**

For detection of  $\text{NO}_3^-$  ion present in aqueous solution, coordination complex formation method has been tried and consequent emission intensities changes have been perceived. Several concentrations (0–14 mM) of  $\text{NO}_3^-$  solutions were used for the purpose of complex formation. As displayed in **Figure 4**, the intensities of the emission spectra of the PANI/Ag were found to decrease with the addition of nitrate ion. The decrease in intensities indicated that the sensor sites excited at the specific excitation wavelengths interacted with  $\text{NO}_3^-$  molecule and the interactions led to the decrease in the emission intensity. In addition, the red shifting of the excitation spectra at low concentration may be due to electron density changes caused by the complexation of  $\text{NO}_3^-$  and a conformational change in the sensor backbone as a result of the chelation. The emission intensity of the PANI/Ag was found to decrease as the concentration of the  $\text{NO}_3^-$  increased up to 14 mM. More increase in the concentration of  $\text{NO}_3^-$  did not cause a further decrease in the emission intensity. This indicate that of the all interaction sites of the sensor are occupied by  $\text{NO}_3^-$  molecules. Therefore, has no sites to interact with additional  $\text{NO}_3^-$  ion. From this data 14 mM of nitrate ion was optimum concentration.

### 3.3.2. Influence of pH

The influence of pH on the quenching emission intensity of PANI/Ag by nitrate ion was described in **Figure 5** below. The PANI/AgNPs showed significant notice-able effects with the change in pH. The shift to lower intensity, as well as the relative intensity ratio values decrease on going from pH 2 to pH 4. This is due to the complexation of  $\text{NO}_3^-$  ions hindered because the necessary lone pair electrons are occupied by protons thereby weak interaction persists, resulting in a low quenching efficiency.

As the pH increased, the fluorescence intensity significantly decreased due to the high quenching efficiency and maximum quenching was observed at pH 6. This is due to the deprotonation of the interaction site, which increases the covalent bond strength between the sensor and nitrate ion. As the pH further increases for basic condition, since competitive metal hydroxide formation, it resulted in a distinct increase in fluorescence intensity resulting in a poor interaction with the sensor. Therefore, pH 6 is recommended as the optimal pH value for further detection.

### 3.4. The Sensitivity of the Detection System

Under the above optimal conditions, the fluorescence intensity of PANI/Ag was found to be such that quenching and the Stern-Volmer fluorescence intensity ratio ( $F_0/F$ ) show a linear diminish with the increasing the nitrate ion is also linearly related with a concentration of 1-14 mM as shown in **Figure 6**. The experiments showed that the nitrate ion concentration is inversely proportional to fluorescence intensity, and gave a good linear change in Stern-Volmer fluorescence emission intensity ratio. In order to clarify the favorable condition for the PANI/Ag to interact with the nitrate ion molecules, quenching efficiency at excitation wavelength was determined using a Stern-Volmer plot. The equation of the Stern-Volmer plot is as given below.

$$I_0/I = 1 + K_{SV} [Q]$$

In a fluorescent sensor, the emission intensity ratio can be defined as the response of the sensor. The sensing capability of the PANI/Ag was revealed from the slopes of the linear plots, which

were corresponding to the quenching rate constants ( $K_{SV}$ ). From the calibration curve, it can be described that the linear dependence of the emission intensity on the concentration of nitrate ion. A linear relationship with the coefficients of regression of 0.996. The calculated  $K_{SV}$  value for the PANI/Ag fluorescent sensor for detection of nitrate ion were found to be  $2.22 \times 10^2 \text{ M}^{-1}$ .

In order to determine the limit of detection of the sensor, the reproducibility of the PANI/Ag at the linear range was investigated at three repetitions. As Figure 6 shows the reproducibility of the PANI/Ag sensor for each concentration of nitrate ions. The LOD of the sensor for nitrate ion determined from the standard deviation of the response at the intercept of the regression line and the value of the  $K_{SV}$ , using the equation below.

$$\text{LOD} = \frac{3 \times SD}{K_{SV}}$$

The limit of detection of the proposed fluorescent sensor for nitrate ion were found to be  $8.9 \times 10^{-4} \text{ M}$ . The detection limit in this case was also good compared with those of the other fluorophore based fluorescent sensing methods as described below.

Sensing material	Linear range	LOD (M)	Reference
EDTA-AgNPs	0 -2.5 $\mu\text{g mL}^{-1}$	$1.8 \times 10^{-4}$	[30]
CN	0 -1800 $\mu\text{M}$	$2.61 \times 10^{-7}$	[21]
GO	0-10 mM	-	[31]
PANI/Ag	0-14 mM	$8.9 \times 10^{-4}$	<b>This work</b>

### 3.5. Selectivity Test

The selectivity of PANI/Ag for nitrate ion detection was performed by adding the same amount of interferences ( $\text{SO}_4^{2-}$ ,  $\text{HCO}_3^-$ ,  $\text{Cl}^-$  and  $\text{OH}^-$ ) into the system. The extent of interference for each anion was shown in **Figure 7**. This result confirms that the detection of nitrate ion by PANI/Ag fluorescent sensor were mostly not influenced by the above interference ions. However, the co-existence of polyatomic anions such as  $\text{SO}_4^{2-}$  and  $\text{HCO}_3^-$  resulted in higher efficiency than other. Therefore, the sensing performance would be slightly affected in the presence of these ions.

### 3.6. Recovery test

The cabbage samples were spiked with different concentration of nitrate ion solutions. By using the calibration curves plotted for the known standard solution (spiked) of nitrate ion, the unknown (found) concentration of nitrate ion (value of X) was successfully calculated by using equation  $y = A + B \cdot X$  obtained from the calibration curves of the standard solution. Therefore, the value of “A” is intercept and B (slope) and the value of y ( $F_0/F$ ) was obtained from the fluorescence recorded for nitrate ion for respective samples. The result indicated a good linear relation between  $F_0/F$  and the spiked concentrations of nitrate ion with coefficient of regression  $R^2 = 0.991$  ( $n = 3$ ), respectively as described in **Figure 8** below. The result confirms that the found values is agreed well with the spiked amount. The obtained recoveries were summarized in Table 1 below, which demonstrates that the proposed method is valid and denoting no serious interferences in the samples. In addition, the RSD were less than 5 %, suggesting a high precision of the proposed method.

#### 4. CONCLUSION

The a new and simple PANI/Ag fluorometric sensing probe for  $\text{NO}_3^-$  detection has been successfully synthesized by polymerization of polyaniline into the surface of Ag NPs. The prepared materials were characterized by using FT-IR, XRD and UV-Visible spectroscopy. The results of the analysis indicated that there is a strong interfacial interaction between polyaniline and Ag NPs. The developed sensor employed as a highly effective tool for selective detection of  $\text{NO}_3^-$  ions present in aqueous solution was based on quenching in the emission intensities resulting from complex formation of the sensor molecule with nitrate ion. The effect approves, the nitrate ion effectively quenched the emission and excitation intensity of PANI/Ag. The dynamic and static quenching mechanisms are show a significant role in the interaction of nitrate ion with the sensing sites of the developed sensor. The developed PANI decorated Ag NPs have their suitability of simple operation and distinct types of optical responses observed, that is due to high surface-area-to-volume ratio. The sensor revealed a linear range, a high selectivity and sensitivity with a low detection limit of  $8.9 \times 10^{-4}$  M.

## **ACKNOWLEDGMENTS**

I would like to express my deepest appreciation and thanks to Mekdela Amba University, Wollo University for providing instruments and laboratory facilities from the beginning to the completion of this study and AAU for FT-IR and XRD analysis.

#### 4. REFERECES

- [1] Wang, L., Ma, W., Xu, L., Chen, W., Zhu, Y., Xu, C. and Kotov, N. A. 2010. Nanoparticle-based environmental sensors. *Material Science Engineering*, 70 : 265 – 274.
- [2] Namasivayam, C. and Sageetha, D. 2005. Removal and recovery of nitrate from water by ZnCl<sub>2</sub> activated carbon from coconut coir pith, and agricultural solid waste. *Indian Journal of Chemical Technology*, 12: 513- 521.
- [3] Braverman, L.E., He, X., Pino, S., Cross, M., Magnani, B., Lamm, S.H., Kruse, M.B., Engel, A., Crump, K.S. and Gibbs, J.P. 2005. The effect of perchlorate, thiocyanate, and nitrate on thyroid function in workers exposed to perchlorate long-term. *The Journal of Clinical Endocrinology & Metabolism*, 90 (2): 700-706.
- [4] Niedzielski, P., Kurzyca, I. and Siepak, J. 2006. A new tool for inorganic nitrogen speciation study: Simultaneous determination of ammonium ion, nitrite and nitrate by ion chromatography with post-column ammonium derivatization by Nessler reagent and diode-array detection in rain water samples. *Analytica Chimica Acta*, 577 (2): 220-224.
- [5] Pourreza, N. and Hoveizavi, R. 2005. Simultaneous preconcentration of Cu, Fe and Pb as methylthymol blue complexes on naphthalene adsorbent and flame atomic absorption determination. *Analytical Chemistry Acta*, 549: 124–128.
- [6] Chaiyo, S., Chailapakul, O., Sakai, T., Teshima, N. and Siangproh, W. 2013. Highly sensitive determination of trace copper in food by adsorptive stripping voltammetry in the presence of 1, 10-phenanthroline. *Talanta*, 108: 1- 6.
- [7] Auffan, M., Rose, J., Bottero, J. Y., Lowry, G. V., Jolivet, J. P. and Wiesner, M. R. 2009. Towards a definition of inorganic nanoparticles from an environmental, health and safety perspective. *National Nanotechnology*, 4: 634 – 641.
- [8] Wang, Z. and Ma, L. 2009. Gold nanoparticle probes. *Coord. Chemical Review*, 253: 1607 – 1618.
- [9] Ma, X. F., Mang, W., Li, G., Chen, H. Z. and Bai, R. 2006. Preparation of polyaniline-TiO<sub>2</sub> composite film with in situ polymerization approach and its gas-sensitivity at room temperature. *Materials Chemistry and Physics*, 98: 241-247.

- [10] Masoumi, V., Mohammadi, A., Amini, M., Khoshayand, M. R. and Dinarvand, R. 2014. Electrochemical synthesis and characterization of solid-phase microextraction fibers using conductive polymers: application in extraction of benzaldehyde from aqueous solution. *Journal of Solid State and Electrochemicals*, 18: 1763-1771.
- [11] Sharma, S., Nirkhe, C., Pethkar, S. and Athawale, A. A. 2002. Chloroform vapour sensor based on copper/polyaniline nanocomposite. *Sensors and Actuators B: Chemical*, 85 (1-2): 131-136.
- [12] Draman, S.F.S., Daik, R. and Ahmad, M. 2009. Synthesis and studies on fluorescence spectroscopy of CSA-doped polyaniline solution in DMF when exposed to oxygen gas. *Malaysian Polymer Journal*, 4 (1): 7-18.
- [13] Maiti, S., Barman, G. and Konar, L. J. 2014. Biosynthesized Gold nanoparticles as catalyst. *International Journal of Scientific and Engineering Resource*, 5(7):1229–1230.
- [14] Misra, T.K. and Liu, C.Y. 2009. Surface-functionalization of spherical silver nanoparticles with macrocyclic polyammonium cations and their potential for sensing phosphates. *Journal of Nanoparticle Research*, 11 :1053–1063.
- [15] Wang, Q. and Yu, C. 2009. Chemical and biological sensing and imaging using plasmonic nanoparticles and nanostructures. *In: Biomedical nanosensors*, 2012:59–96.
- [16] Qu, L. H., Peng, Z. A. and Peng, X. G. 2001. Alternative routes toward high quality CdSe nanocrystals. *Nano Letters*, 1 :333 – 337.
- [17] Koh, I., Hong, R., Weissleder, R. and Josephson, L. 2008. Sensitive NMR sensors detect antibodies to influenza. *Angew. Chem. Int. Ed. Engl.* , 47 : 4119 – 4121.
- [18] Zhang, J., Lei, J., Xu, C., Ding, L. and Ju, H. 2010. Carbon nanohorn sensitized electrochemical immunosensor for rapid detection of microcystin-LR. *Analytical Chemistry*, 82: 1117 – 1122.
- [19] Maiti, S., Barman, G. and Konar Laha J. 2016. Detection of heavy metals ( $\text{Cu}^{+2}$ ,  $\text{Hg}^{+2}$ ) by biosynthesized silver Nanoparticles. *Applied Nanoscience*, 6:529–538.
- [20] Bisetty, K., Sabela, M.I., Khulu, S., Xhakaza, M. and Ramsarup, L. 2011. Multivariate optimization of voltammetric parameters for the determination of total polyphenolic content in wine samples using an immobilized biosensor. *International Journal of Electrochemical*, 6: 3631-3643.

- [21] Alim, N.S., Lintang, H.O. and Yuliati, L. 2015. Fabricated metal-free carbon nitride characterizations for fluorescence chemical sensor of nitrate ions. *Journal of Technolodge (Sciences & Engineering)*, 76 (13): 1-6.
- [22] Silva, R.F. and Zaniquelli, M.E.D. 2002. Morphology of nanometric size particulate aluminium-doped zinc oxide films. *Colloid Surface A*, 551: 198.
- [23] Song, J.Y., Jang H.K. and Kim, B.S. 2009. Biological synthesis of gold nanoparticles using *Magnolia kobus* and *Diospyros kaki* leaf extracts. *Process Biochemistry*, 44(10):1133–1138.
- [24] Niu, Z., Z. Yang, Z. Hu, Y. Lu, C.C. Han. 2003. Polyaniline-Silica Composite Conductive Capsules and Hollow Spheres *Adv. Funct. Mater.*, 13: 949-954.
- [25] Ayad, M. M., Salahuddin, N. A., Minisy, I. M. and Amer, W. A. 2014. Chitosan/ polyaniline nanofibers coating on the quartz crystal microbalance electrode for gas sensing. *Sensor Actuators B*, 202: 144-153.
- [26] Sonker, R.K. and Yadav, B.C. 2017. Development of Fe<sub>2</sub>O<sub>3</sub>–PANI nanocomposite thin film based sensor for NO<sub>2</sub> detection. *Journal of the Taiwan Institute of Chemical Engineers*, 77: 276-281.
- [27] Gu, L., Wang, J., Qi, R., Wang, X., Xu, P. and Han, X. 2012. A novel incorporating style of polyaniline/TiO<sub>2</sub> composites as effective visible photocatalysts. *Journal of Molecular Catalysis A: Chemical*, 357: 19-25.
- [28] Melaku Wondwossen, Yadav, OP. and Kebede Tesfahun. 2014. Photo-catalytic Removal of Methyl Orange Dye by Polyaniline Modified ZnO using Visible Radiation. *Science Technology and Arts Research Journal*, 3(2): 93-102
- [29] Singh, S., Rama, N. and Rao, M. S. R. 2006. Influence of d–d transition bands on electrical resistivity in Ni doped polycrystalline ZnO. *Applied Physics Letter*, 88 (22): 222111-222113.
- [30] Wang, C.C., Luconi, M.O., Masi, A.N. and Fernández, L.P. 2009. Derivatized silver nanoparticles as sensor for ultra-trace nitrate determination based on light scattering phenomenon. *Talanta*, 77(3): 1238-1243.
- [31] Tang, H., Sundari, R., Lintang, H.O. and Yuliati, L. 2016. Detection of nitrite and nitrate ions in water by graphene oxide as a potential fluorescence sensor. *In IOP Conference Series: Materials Science and Engineering*, 107: 012027.

## Figure Caption

Figure 1. FT-IR spectra of PANI/Ag nanocomposite

Figure 2. XRD patterns of the as-synthesized nanocomposites (where A: Ag NPs, B: PANI, AB: PANI/Ag).

Figure 3. UV-vis DRS analysis of the as-synthesized composites.

Figure 4. Emission spectrum of PANI/Ag upon addition of  $\text{NO}_3^-$  ion with various concentration.

Figure 5. Effect of pH

Figure 6. The reproducibility of the PANI/Ag responses for  $\text{NO}_3^-$  ion concentration

Figure 7. Fluorescence responses of PB = PANI/Ag (left bar) after treatment of 14 mM  $\text{NO}_3^-$  ion solutions, and interference of 14 mM of other anions with 14 mM  $\text{NO}_3^-$  ion (right bar).

Figure 8. Calibration curve of  $F_0/F$  Vs. different concentration of nitrate ion spiked samples

**Table Caption**

Table 1. Detection of nitrate ion in cabbage samples by spiked method (n = 3).

Figure 1

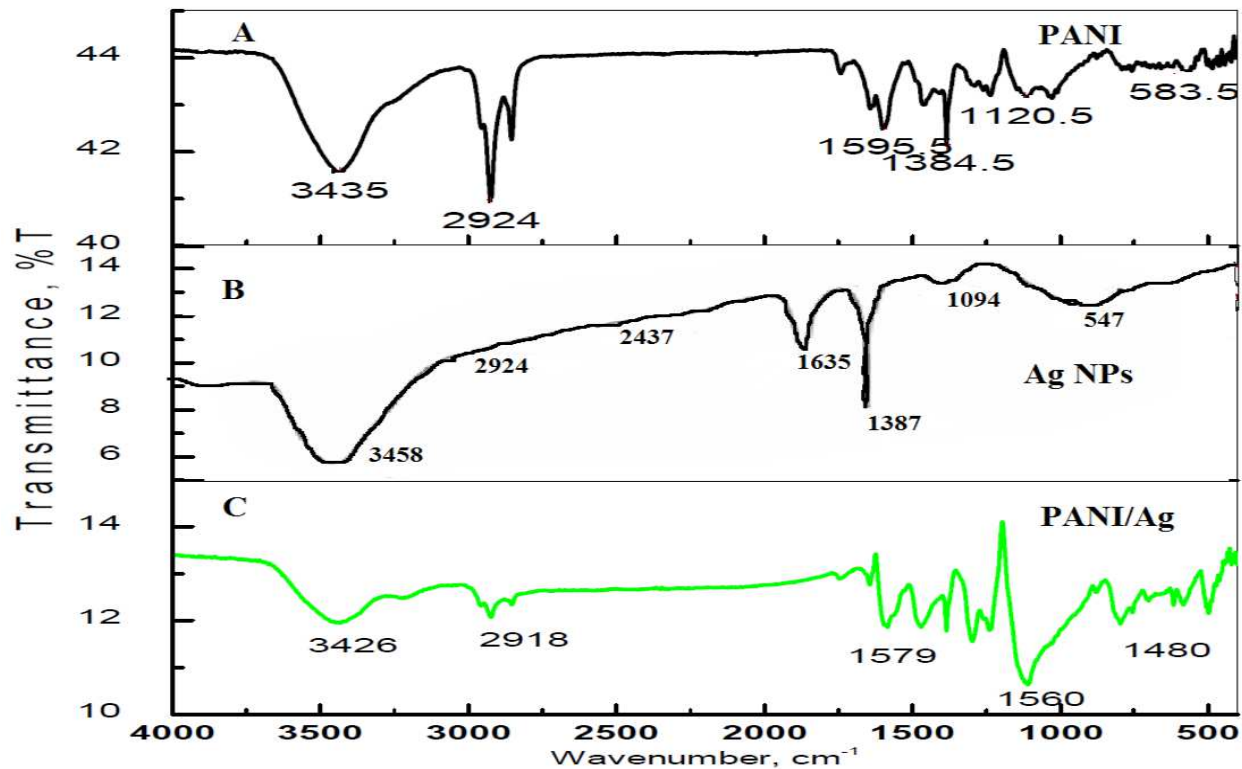


Figure 2

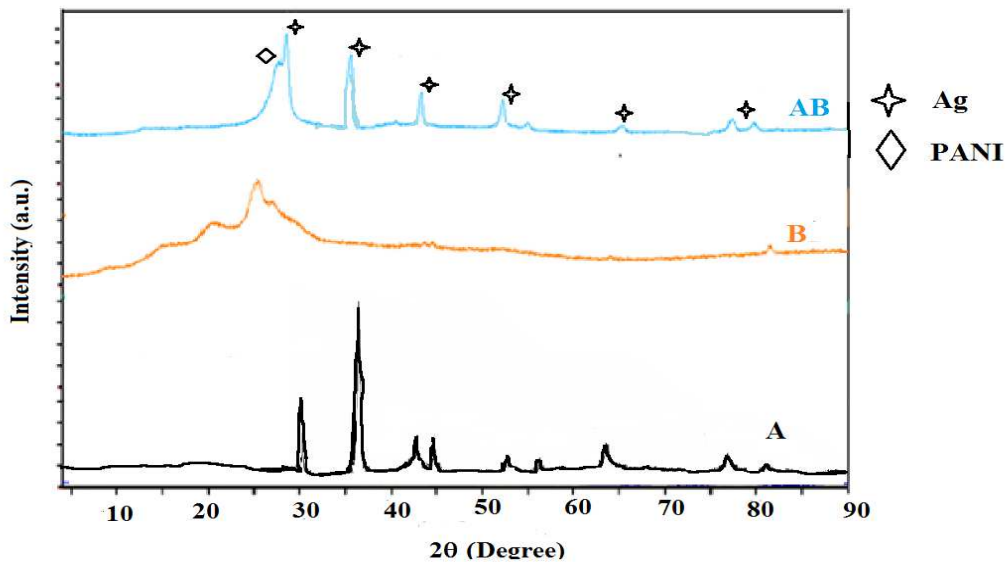


Figure 3

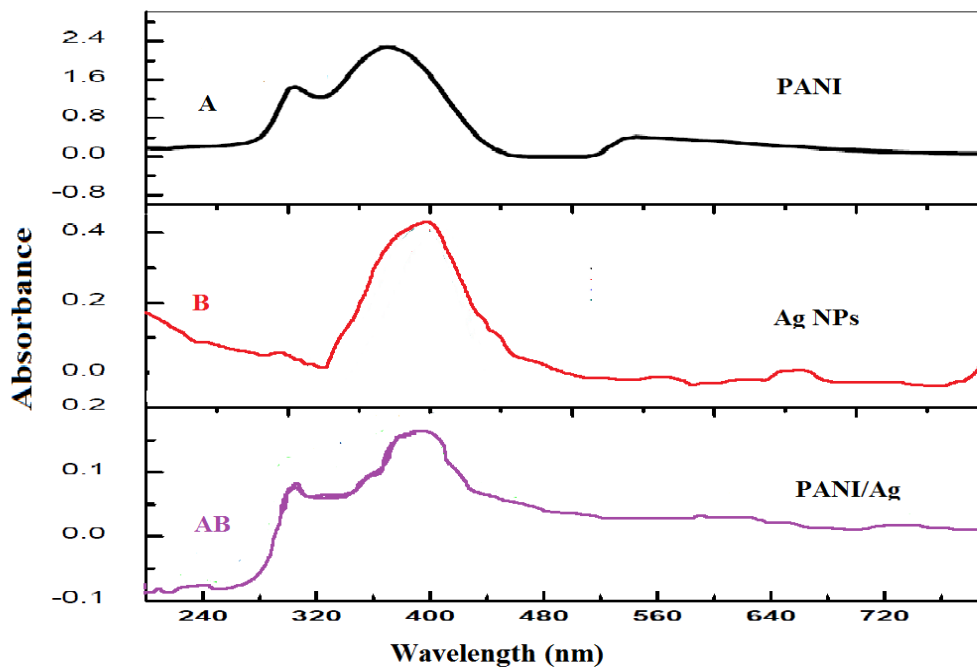


Figure 4

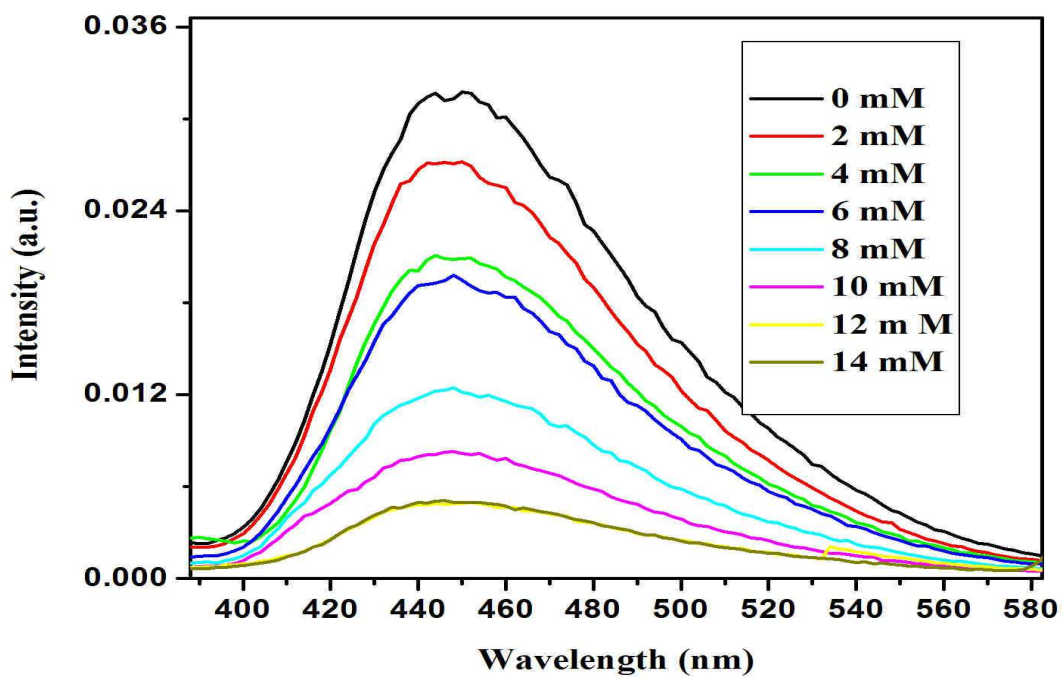


Figure 5

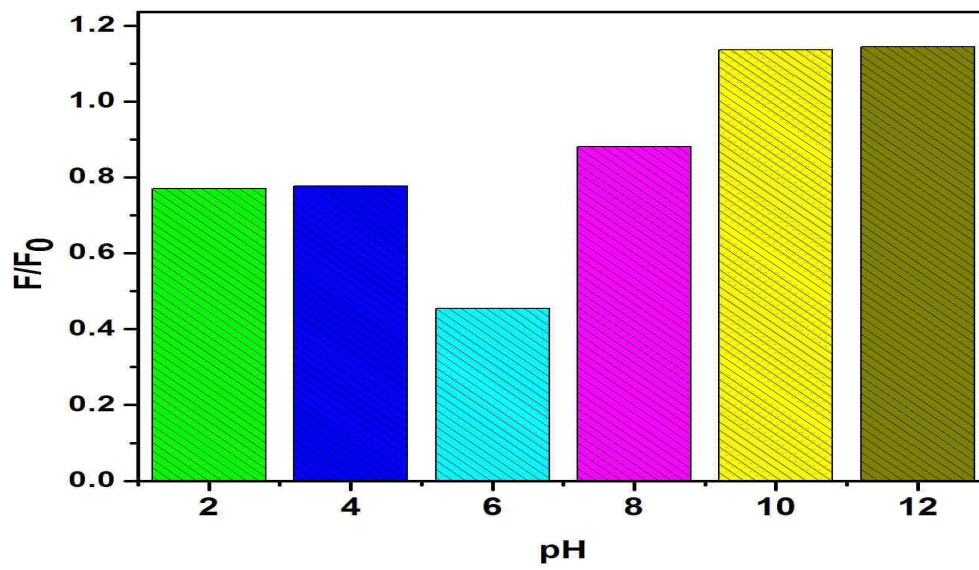


Figure 6

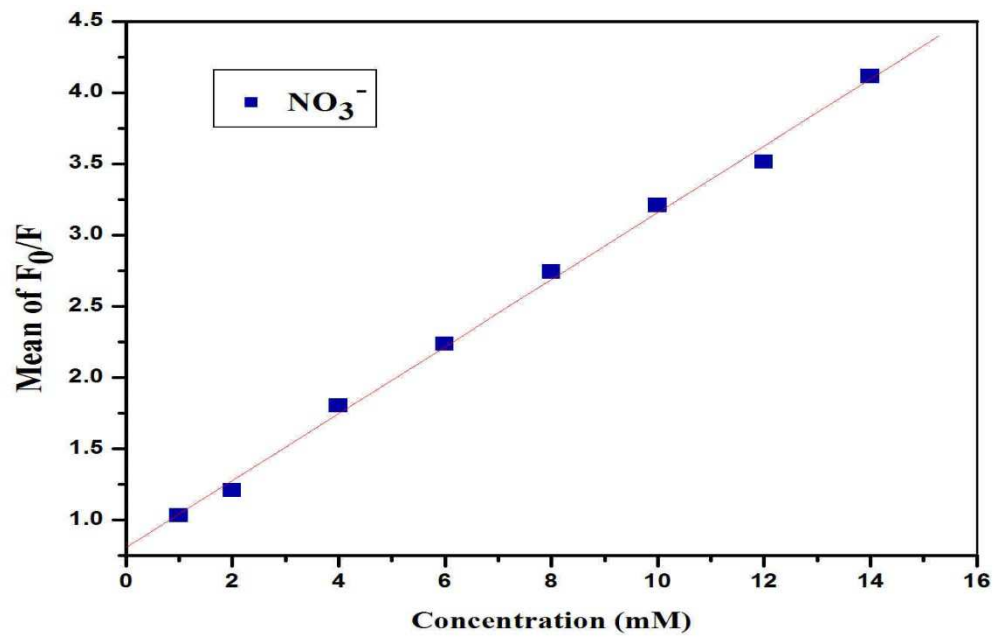


Figure 7

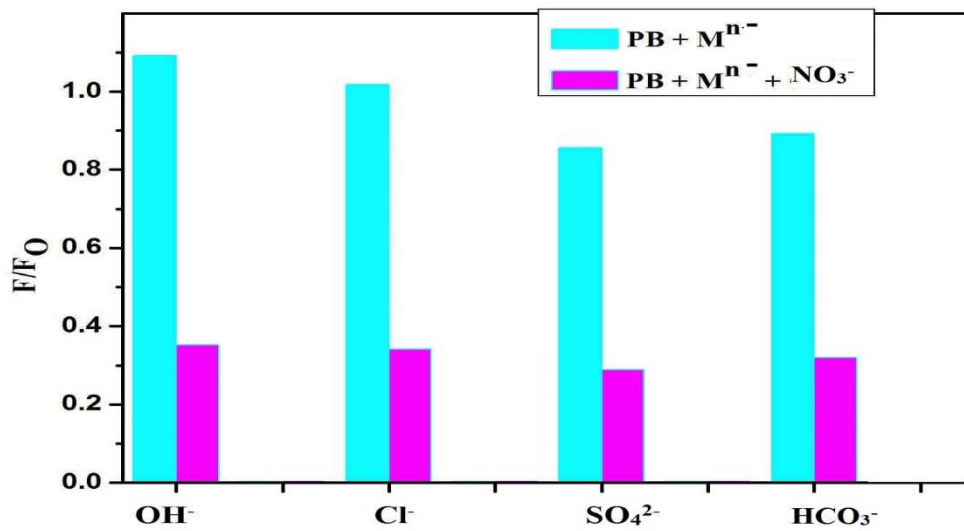
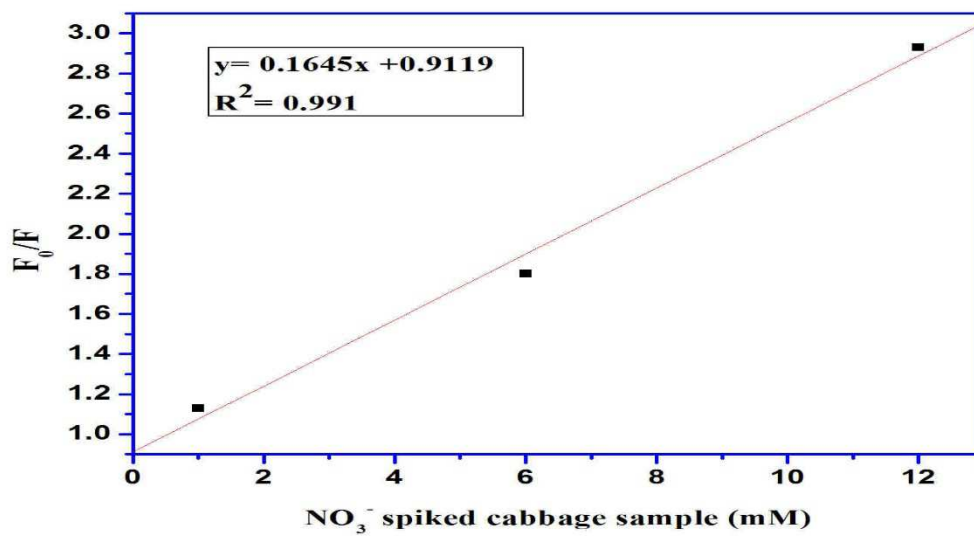


Figure 8



**Table 1**

Samples	Added (mM)	Found (mM)	Mean recovery (%) <sup>a</sup>	RSD (%)
1	1	1.032	103.2	1.04
2	6	5.41	90.1	2.7
3	12	12.26	102.1	4.2